724 *Chem. Mater.* **2010,** *22,* 724–739
DOI:10.1021/cm9030478

CHEMISTRY OF MATERIALS
Review

Hunting for Better Li-Based Electrode Materials via Low Temperature Inorganic Synthesis†

Jean-Marie Tarascon,* Nadir Recham, Michel Armand, Jean-Noël Chotard, Prabeer Barpanda, Wesley Walker, and Loic Dupont

Laboratoire de Réactivité et Chimie des Solides, Université de Picardie Jules Verne, CNRS UMR6007, 33 rue Saint Leu, 80039, Amiens, France

Received October 1, 2009. Revised Manuscript Received November 17, 2009

Ceramic processes are currently used to prepare most of today's electrode materials. For energy-saving reasons, there is a growing interest in electrode materials prepared via eco-efficient processes, which has led to the resurgence of low temperature hydro- and solvothermal processes. This review will highlight how some of these processes have been successfully used to prepare today's most praised electrode material: $LiFePO_4$. Particular attention is paid to the recently developed ionothermal synthesis process. This will be done in order to stress the versatility and richness of ionothermal synthesis, its control over particle size and shape, and the ability of ionic liquids to provide stabilization to new metastable phases. We outline the pertinent questions that should be clarified for continued advancement of the ionothermal process which opens the door to innovative inorganic synthesis and to materials which have remained hidden for a long time.

Introduction

Global warming, finite fossil-fuel supplies, and city pollution conspire to make the use of renewable energies (wind, tidal, wave, solar) and the replacement of petroleum with electric propulsion a worldwide imperative.[1,2] However, better energy storage systems must be developed because road transport electrification requires stored power onboard, and renewable energies require, owing to the intermittence of their outputs, storage assistance to ensure a continuity of supply. Among the various available storage technologies, the Li-ion battery,[3] which has conquered the portable electronic market, has become the prime candidate to power the next generation of Electric Vehicles (EVs) and Plug-in Hybrid Electric Vehicles (PHEVs) and stands as a serious contender for small scale decentralized applications such as photovoltaics.

There are several reasons why Li-ion batteries should meet great success in these emerging markets. First, Li-ion cells offer the largest energy density and output voltage of all known rechargeable battery technologies. Moreover, Li-ion technology relies on a rich and versatile chemistry[4] leading to a wide range of attractive electrode materials for both positive ($LiCoO_2$, $LiMn_2O_4$, $LiFePO_4$) and negative electrodes (C, Sn, Si, etc.), and this list does not include the candidates from the organic world. In contrast, competing technologies like lead−acid and Ni−Cd offer a single redox couple or are often pinned-down to a single positive electrode (NiOOH for Ni-MH technology). Owing to this strong dependence on materials to dictate performance, it does not come as a surprise that solid-state chemistry has played a central part in the rapid development of the Li-ion technology, whose existence relies on the discovery of Li-insertion compounds back in the 1970s[4−7] and continues so that new materials (phosphates,[8] silicates,[9] borates[10]), new electrode reactions (conversion,[11] displacement reactions[12]), and rethought synthetic processes (solvothermal,[13,14] ionothermal[15,16]) are brought on to the scene, widening the type of Li-ion redox couples and the type/nature and morphology of the electrodes. Owing to the latter, and the great amount of effort devoted to nanoparticles, nanocomposites, nanoporous materials, nanotextured/nanostructured electrodes, and nano-architectured current collectors,[17,18] Li-ion technology is presently enjoying, a few decades after the field of microelectronics, its "nanomania" with exciting opportunities. Solid-state chemistry with its ability to manipulate, shuffle atoms, and control particle growth−surface morphology has been keen in promoting this recent paradigm shift from bulk to nanomaterial electrodes, which has a considerable impact on current battery performances.

The constant interlink between materials and their applications has driven the field of inorganic synthesis over the years, and this trend will continue into the future. While the hunt for high performance electrode materials for Li-ion batteries remains the main research objective, cost associated with producing these materials is now becoming another overriding factor. Notions of sustainability, renewability, and green chemistry must be taken into consideration when selecting electrode materials for the next generation of Li-ion cells, especially when designing materials for high volume applications.[19] This

† Accepted as part of the 2010 "Materials Chemistry of Energy Conversion Special Issue".

*Corresponding author. E-mail: jean-marie.tarascon@sc.u-picardie.fr.

 Published on Web 12/30/2009

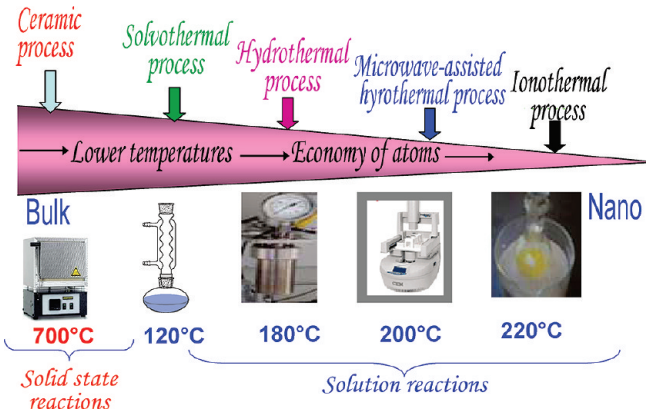

Figure 1. Summary of the recent synthesis approaches toward the preparation of highly divided $LiFePO_4$ powders taking into account energy and material thrift.

constitutes an open call for the development of novel eco-efficient synthetic processes aimed toward modifying existing electrode materials or developing new ones. Most of today's electrode materials ($LiCoO_2$, $LiNi_{1/3}Mn_{1/3}Co_{1/3}O_2$, $LiMn_2O_4$) are made via high temperature solid-state reactions; a widely utilized approach referred to as the "ceramic process" which consists in reacting, at various temperatures and pressures, two solids A and B to form a third one AB via local mass transport. Due to the low diffusion coefficient in solids, the traditional solid-state reaction requires high thermal activation along with lengthy annealing times, which render the ceramic approach energetically demanding. Additionally, this approach excludes the preparation of low temperature metastable phases and precludes any rational control over particle morphology.

To eschew some of the above difficulties and broaden their degree of freedom by preparing both metastable phases and affecting particle morphology, researchers presently favor low temperature synthetic methods grouped under the name "Chimie douce",[20] in order to make the next generation of electrode materials. Powders of $LiFePO_4$, currently the most studied electrode material for EVs applications, are synthesized in such a way as to give homodispersed nanosized powders via low temperature hydrothermal processes. However, this material requires a post treatment of 700 °C in order to make carbon nanopainting;[21] so many argue that $LiFePO_4$ is not made at low temperatures!

This return to low temperature chemistry, driven by the energy crisis, has rekindled the positive attributes of the hydro- and solvothermal synthetic processes, rejuvenated past synthesis strategies such as the use of a "latent base" which had fallen into oblivion, and triggered the advent of new synthetic approaches such as ionothermal synthesis (Figure 1). This review will feature some of the aforementioned low temperature methods, how they have been used to manipulate the morphology of known electrode materials, and unravel new metastable electrochemically active phases never reported before. Due to space limitations, we will limit descriptive examples of the solvothermal and latent base processes in order to devote more time to ionothermal synthesis and more so how it applies to the field of inorganic chemistry. For comparative purposes, throughout the first part of this review, our examples will be primarily devoted to the synthesis of $LiFePO_4$ and then will be extended to a wide class of materials including Na- and F-based polyanionic compounds. This review will conclude with a look at future synthetic trends, some of which involve biomineralization approaches.

Synthesis of $LiFePO_4$ via Low Temperature Processes. $LiFePO_4$ (denoted hereafter as LFP), which is a natural mineral known as triphylite, has recently been intensively studied because of its low cost, minimal environmental impact, and enhanced safety associated with its redox voltage (3.45 V vs Li/Li^+) falling within the thermodynamic range of most of the electrolytes presently used in Li-ion cells. Initially LFP was not a favorite as potential material for use in electrodes because it has both poor electronic and ionic conductivities; however, these negative attributes have been overcome by applying (Figure 2) nanosizing[14] and carbon nanopainting techniques[21] to the synthesis of LFP electrodes. Despite the fact that $LiFePO_4$ is a mineral, mining is not an option considering the purity and the nanometric aspects of the required powders, so synthetic triphylite powders have to be made, aiming at grain sizes that can be directly processed into electrode materials, via the most expeditious and energy-saving processes, in order to preserve the low inherent cost of the mineral. Increasingly, ceramic approaches combined with postgrinding steps in the presence of carbon, to decrease particle size and achieve electronic carbon conducting matrices, are being abandoned in favor of low temperature solution routes.

Aware of this situation, chemists have revisited mild temperature hydro- and solvothermal processes, which enlist precipitation reactions and have been successfully used in the past for the synthesis of numerous inorganic compounds. More specifically, a typical solvothermal reaction consists of reacting, in a liquid medium, the corresponding metal/nonmetal based soluble salt precursors with the proper bases at a temperature sufficient enough to promote the precipitation and growth of the desired phase via Ostwald ripening.[22] Hydrothermal reactions require harsher experimental conditions because they are performed under pressure. Using pressure as another experimental variable allows control over precipitation kinetics and the precipitation of metastable phases.

Back in 2001, Whittingham et al.[23] were the first to show that LFP could be formed by a hydrothermal process relying on the following reaction [$H_3PO_4 + FeSO_4 + \mathbf{3LiOH} \rightleftharpoons LiFePO_4 + \mathbf{Li_2SO_4} + 3H_2O$]. However, owing to both, some inversion between Fe and the lithium sites and the presence of small amounts of $Fe^{(III)}$ in the synthesized compound, the resulting electrodes showed poor electrochemical performances. The addition of L-ascorbic acid to their reaction mixtures in order to reduce the ferric iron and carbon nanotubes to enhance electronic percolation between particles allowed the authors to successfully synthesize LFP/C composites

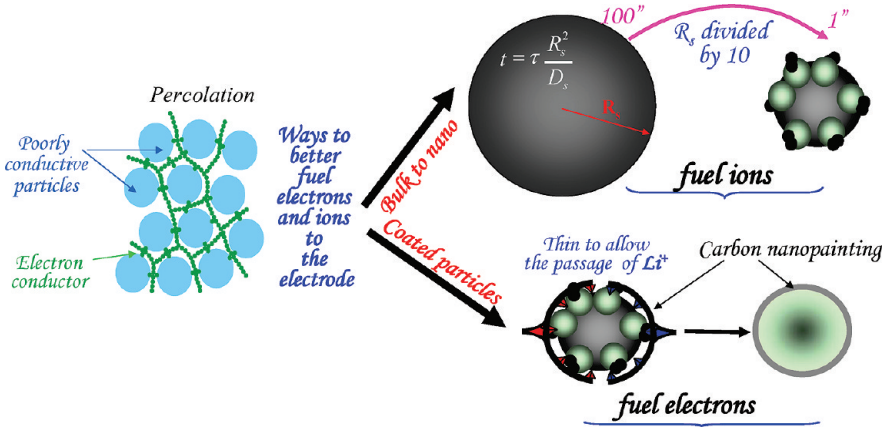

Figure 2. Schematic of electrode wiring so as to stress the importance of both downsizing the particle size and carbon nanopainting to improve electrode kinetics when poorly conducting electrochemically active materials are used.

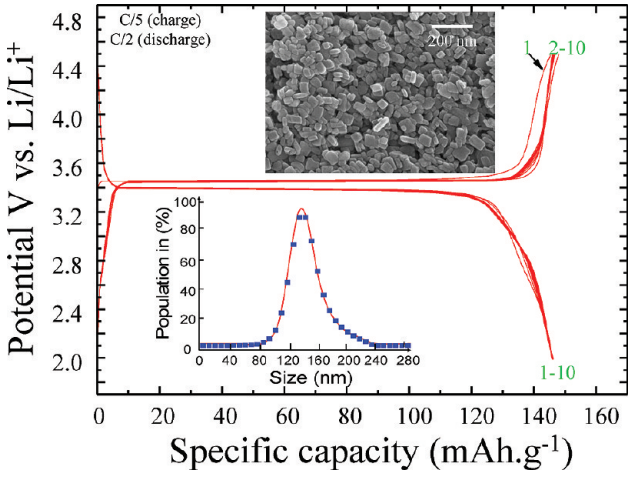

Figure 3. The electrochemical performances of solvothermally prepared $LiFePO_4$ powders together with, as insets, their particle size distribution (bottom left corner) and their scanning electron microscope (SEM) image (top right corner). The active material was mixed with 5% of carbon and a loading of 3 mg of active material per squared centimeter was used.

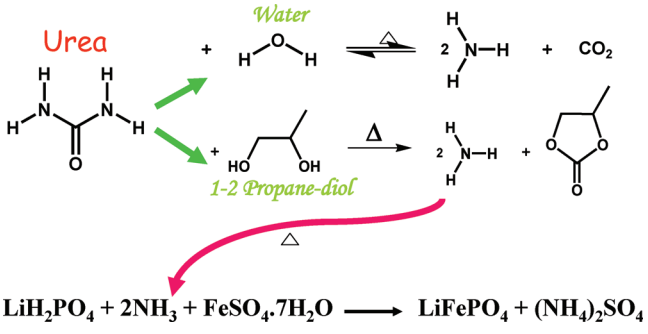

Figure 4. Chemical reactions describing the concept of latent bases. The decomposition of urea into NH_3 upon mild heating conditions is shown in both water and diol media.

that were able to deliver sustainable capacities of 145 mAh/g.[13] Using the same precursors but with the clever addition of DMSO to water in order to increase the boiling point to about 120 °C, Delacourt et al.[14] succeeded, via a precipitation process under reflux, in making homogeneous 140 nm Li_xFePO_4 powders. Furthermore, the powders were able to sustain reversible capacities of 145 mAh/g at C/2 rates (Figure 3) without the need of a carbon coating after a short annealing time at 500 °C under a reducing atmosphere of N_2/H_2 to fully dehydrate the material and reduce $Fe^{(III)}$ impurities.

While both aforementioned methods can provide high quality monodispersed powders and be easily scaled up to tonnage quantities, they present some mild drawbacks linked to the fact that (1) local precipitation of $Fe(OH)_2$ by LiOH is necessary, leading to air oxidized $Fe^{(III)}$ impurities in the final product and causing previous authors to either add ascorbic acid to their solution or postheat their precipitated powders and (2) they require the use of costly LiOH, two-thirds being turned into useless Li_2SO_4, failing to maximize the economy of atoms, and generating Li_2SO_4 as a hardly recoverable side product.

To address these issues, our group[15] has pursued the concept of "forced hydrolysis", a process pioneered by Matijevic et al.[24−26] back in the late 1990s, to hydrothermally prepare $Fe^{(III)}$-free LFP powders according to the following reaction [LiH_2PO_4 + urea + $FeSO_4 \cdot 7H_2O \rightarrow$ $LiFePO_4$ + $(NH_4)_2SO_4$ + CO_2 + $7H_2O$]. This process which avoids the use of LiOH (Figure 4) rather relies on the use of urea as an initially neutral chemical which upon mild heating liberates the basic species (NH_3) needed to complete the precipitation reaction. Besides it leads to an innocuous byproduct (e.g., $(NH_4)_2SO_4$, a fertilizer). Moreover, owing to both the wide variety of latent bases that exist in addition to urea (guanidinium, isocyanate salts, hexamethylenetetramine, etc.) and that are capable of producing in situ basic species, and the range of solvents in addition to water (diols, formamide, dimethylformamide, etc.) capable of triggering the release of the base, "forced hydrolysis" offers countless synthetic opportunities to be implemented in the synthesis of numerous phosphates and silicates.

Microwave-assisted solvo- or hydrothermal processes originally reported by Manthiram et al.[27] and more recently by Novak et al.[28] constitute another attractive route in the eco-efficient synthesis of $LiFePO_4$ powders showing high electrochemical performances (e.g., sustained reversible capacities of 160 mAh/g). These LFP

powders are reported to be synthesized with short reaction times (5 to 10 min) at temperatures < 300 °C and with short (~1 h) post-annealing times at 700 °C under a reducing atmosphere in order to produce effective carbon coating from sucrose, initially introduced with the reaction vessel. With short reaction times, a microwave-assisted solvothermal process stands as an attractive high throughput synthetic method for rapidly screening phase diagrams.

Regardless of the merit of the aforementioned approaches, they still need to be conducted under reflux and controlled environment (e.g., solvothermal process) with the mandatory use of investment intensive autoclaves for hydrothermal processes. Bypassing such a limitation requires the use of nonvolatile reacting media. Along that line, another more recent innovation brought to the scene to prepare LFP, free of the mandatory use of autoclaves or reflux systems, has been the use of ionic liquids, which neither decompose nor exhibit significant vapor pressure up to 300−400 °C. Ionothermal synthesis, widely used in organic chemistry,[29,30] has led to very appealing results and will be the focus of the rest of this review as it applies to either the modification of known materials or in the synthesis of new compounds.

Ionothermal Synthesis

Ionic liquids (referred to hereafter as ILs), which are room temperature molten salts, have recently become key materials in emerging applications within the fields of energy storage devices, biosciences, and biomechanics, in addition to the roles they have played earlier in the electrodeposition of metals and organic synthesis.[31] Therefore, it is surprising that ionic liquids, despite their hundred years of existence, have remained unattractive to inorganic chemists as a synthetic medium. This is quite odd when you consider the fact that molten salt synthetic methods using inorganic melts have been common practice in the field of inorganic synthesis and have led to a wide variety of new oxides and intermetallic phases. The first in-road into the field of solid-state chemistry was recently reported by Morris in 2007.[32−34] In these papers, the authors were able to grow inorganic−organic compounds belonging to the metal−organic-framework family (MOFs) using ionic liquids as the synthetic media. Inspired by this work, we decided to go one step further and fully utilize ionic liquids to synthesize inorganic compounds. There were two main reasons for this: first, like water, ionic liquids resulting from compatible cationic/anionic pairs have excellent solvent properties which enable low temperature processes, and second, they possess high thermal stability and negligible volatility which means that synthesis can be performed without the use of an autoclave. Moreover, they are made of organic cation−anion pairs which provide a practically unlimited number of ionic liquids with different physical−chemical properties (i.e., hydrophobicity, melting point, viscosity, and solvating properties) to choose from to conduct the proper synthesis, while the number of inorganic molten salts is relatively limited.[35]

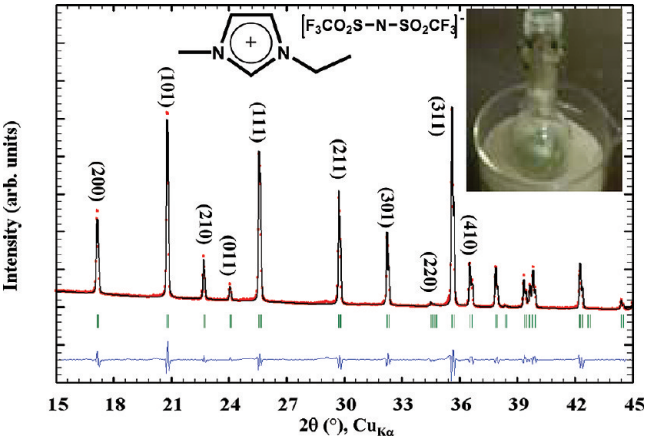

Figure 5. X-ray diffraction pattern collected on $LiFePO_4$ powders prepared using 1-ethyl-3-methylimidazolium bis-(trifluoromethanesulfonyl imide) as the ionic liquid medium.

The first proof-of-principle experiments to validate this novel synthetic pathway have been conducted on LFP.[16] We chose $LiFePO_4$ so that our results could be rapidly benchmarked against a well-trodden electrode material and to determine whether ionothermal synthesis could present some advantages. When choosing among the many ionic liquids that are currently known, we favored ionic liquids that had a high thermal stability, hydrophobicity, and high polarity in order to increase their solvating power toward our reactants. On that basis, we selected (EMI-TFSI) 1-ethyl-3-methylimidazolium bis-(trifluoromethanesulfonyl) imide as the reacting medium to conduct our first experiments and Fe oxalate ($FeC_2O_4 \cdot 2H_2O$) and LiH_2PO_4 as the Fe- and Li-based precursors, owing, based on aqueous data, to their anticipated partial solubility in EMI-TFSI. In a 50 mL flask, 5 mL of EMI-TFSI was added to stoichiometric amounts of $FeC_2O_4 \cdot 2H_2O$ (99%, Aldrich) and LiH_2PO_4 (99%, Aldrich) in the appropriate quantities so as to prepare 0.8 g of $LiFePO_4$. The suspension was then stirred for 10 min, placed into an oven, heated at a rate of 5 °C/min to 250 °C, and maintained at this temperature for 24 h. Under such conditions, single-phase, as deduced by X-ray diffraction (XRD), and greenish $LiFePO_4$ powders (Figure 5) were obtained quantitatively, while 600−700 °C is necessary via the ceramic process, hence adding for the first time ionothermal synthesis as an alternative synthetic path toward the low temperature preparation of inorganic compounds. Additionally, we succeeded in preparing single-phased $LiFePO_4$ from the above reaction mixture in 30 min at 250 °C using microwave rather than thermal heating.

In light of such positive results and in order to grasp further insight into the underlying reaction mechanism, we explored how the use of various ionic liquids could affect both the feasibility of such a reaction and the morphology of the obtained powders. To do so, various ionic liquids which change following the nature of the cations (*pyridinium vs imidazolium*), cations substitutions (*alkyl-chains vs OH or CN termination and methyl groups vs protons on C_2 position*), and the nature of the anion

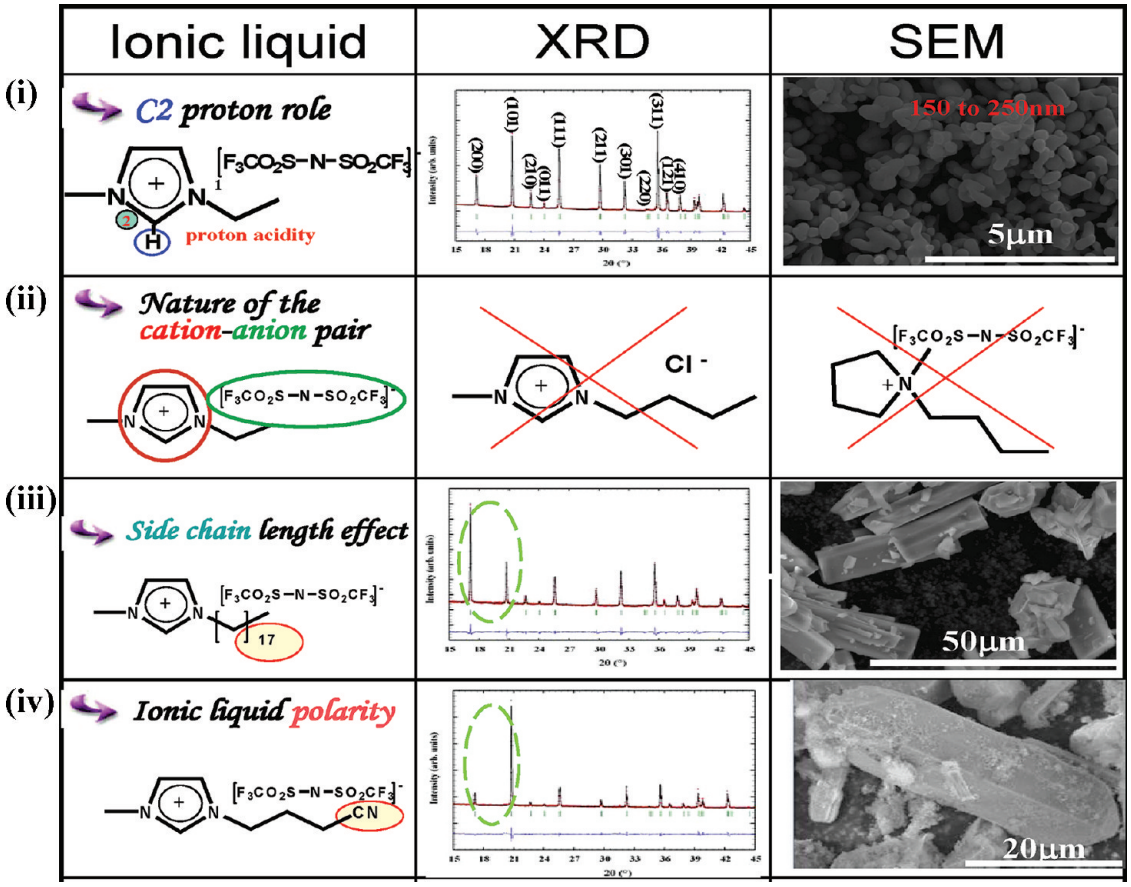

Figure 6. Effect of acting upon the ionic liquid chemistry with (from top to bottom) (i) modifying substituent on the C2 position (proton vs methyl group), (ii) changing the cation−anion pairs (red crosses indicate the cation−anion pairs which do not lead to $LiFePO_4$), (iii) tuning the side chain length, and (iv) adjusting the alkyl-chain termination (CN vs OH) on the morphology of the synthesized $LiFePO_4$ powders, as deduced from XRD and SEM measurements (right two columns).

(*from fluorinated* ($TFSI^-$) *to nonfluorinated* (Cl^-)) were tested, knowing from previous work that, for instance, C_2 protons are very acidic and then labile or that the length of cations alkyl chain affects the ILs polarity with the highest polarities obtained for the shortest chains or chains having appended nitrile, alcohol, or ketone groups (Figure 6).

From this survey,[16] we were able to conclude that a proper choice of anion and cation was essential for a successful synthesis as we could not, under the same conditions (reacting time, temperature, and precursors), synthesize $LiFePO_4$ with ILs having Cl^-, BF_4^-, or $C(CN_3)^-$ instead of $TFSI^-$ anions, or with ILs having pyrrolidinium instead of imidazolium or pyridiniums cations. The reasons for this are twofold. The first one is nested in the lower thermal stability (not beyond 230 °C for some) of such ILs and is due to either anions with large charge density (Cl^- instead of $TFSI^-$) or localized (e.g., pyrrolidinium) vs delocalized (imidazolium) charge on the cation, which prevents from reaching an adequate synthetic temperature. The second reason is nested in the chemical stability of the anions with respect to the LiH_2PO_4 reactants because they formed either HCl (Cl^-) or HF (BF_4^-). However, changing the nature of the precursors ($FeCl_2 + Li_3PO_4$) enabled us to partially bypass some of the above difficulties. In contrast, for the same imidazolium cation, the morphology of the obtained LFP powders was independent of the nature of the C_2 substituant (H or CH_3). Similarly, modifying the alkyl chain length has very little effect on the sample morphology; however, there appears to be a threshold alkyl chain length (C18) beyond which drastic differences were observed (namely, a preferential growth of crystals along the [**200**]). We attributed this effect to the liquid crystal-type behavior for long alkyl chain ILs, which tended to align and serve as a template in the growth of $LiFePO_4$. Nevertheless, the most spectacular morphology change was found to be induced by the nature of the alkyl-chain termination group, with the most prominent effect shown for CN ending chains, which favored powders containing long needlelike single crystals growing along the [**101**] direction. Such an effect is most likely rooted in the strong solvating effect of CN groups for Fe^{II} species as supported by the existence of very stable cyano-complexes $[Fe(CN)_6^{4-}]$.

In order to find some rationale for these above observations, one first needs to obtain further insight into the exact role of the ionic liquid in ionothermal synthesis reactions. Complementary solubility tests, differential scanning calorimetry (DSC) measurements, and high-resolution transmission electron microscopy (HRTEM) studies were conducted.[16] A solubility of 2.2 and 2.6 g/L

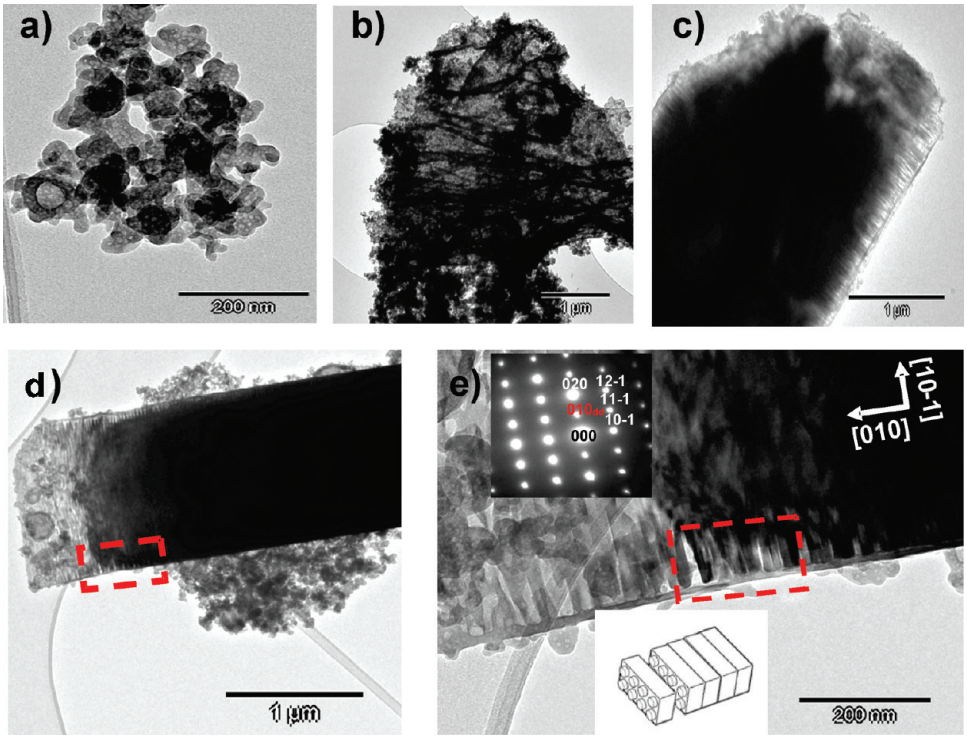

Figure 7. TEM images of a $LiFePO_4$ sample grown in a CN-based ionic liquid highlighting the growth mechanism within the formation of the primary particles (a), their gathering to form thin needles which then stacked together in their longitudinal directions (c and d) in a domino-type mode to form large single crystal fibers (as deduced by the punctual SAED pattern (e)), lying on the (101) plane consistent with the preferential orientation observed by XRD (last row, second column; Figure 6).

at 25 and 100 °C, respectively, was determined for LiH_2PO_4 while $FeC_2O_4 \cdot H_2O$ is only sparingly soluble. DSC measurements on the various components of the mixture, taken individually or when stoichiometrically mixed in the presence or absence of the ionic liquid, were conducted together with an XRD investigation of the final products. We found that the decomposition trace for a **IL-free** $LiH_2PO_4 + FeC_2O_4 \cdot H_2O$ powdered mixture to be the sum of the two DSC curves of the two components collected individually indicating that both precursors are independently decomposing and not reacting in this temperature range as confirmed by the XRD patterns collected on the heated samples. In contrast, in the presence of the ionic liquid, the DSC trace for the $LiH_2PO_4 + FeC_2O_4 \cdot H_2O$ was drastically modified, and the decomposition products were different (as deduced by XRD) suggesting that the ionic liquid plays a key role in the decomposition reaction.

To further complement the nucleation/growth mechanism of $LiFePO_4$, HRTEM microscopy was done on $LiFePO_4$ particles grown in the CN-based ionic liquid,[16] and we could, on the same sample, follow the various steps of the nucleation/growth process as a function of time. At the early stage of the process, there is the formation of 100 nm primary particles (Figure 7a) which gather together to form 1 μm needles (Figure 7b). Then, this growing process appears to stop, most likely due to the surface energy minimization between the tip and lateral needle surfaces, at the expense of a second agglomeration process in which the freshly grown needles pile up in a "Lego"-like fashion to produce micrometer long fibers having the width of the building block length (e.g., needle length) (Figure 7c−e). From their punctual selected area electron diffraction (SAED) patterns (Figure 7e inset), we could deduce that such fibers were single crystals, and that they were laying on the (101) plane consistent with the preferential orientation observed by XRD. On the basis of this observation, it looks like the ionic liquid plays the role of both solvent and surface growth directing template agent during the nucleation and growth stage of the process. This could come as a surprise as we pertinently know that our precursors are sparingly soluble in ionic liquids. So, it is most likely during the IL mediated decomposition step of the precursors that the solubilized reacting species are liberated within the ionic liquid facilitating transport and bringing the reacting species together to trigger phase nucleation. To secure this hand-waving explanation, an in situ high temperature NMR experiment together with semi-in situ analytical measurements (IR, XRD) are presently being designed.

Numerous batches of $LiFePO_4$ powders, which differ in their particles size and morphology, were made via ionothermal synthesis and tested for their electrochemical performances. Samples made of nanosize particles (e.g. those made from EMI-TFSI and containing 300 and 500 nm) were found to perform best with sustainable reversible capacities of 150 mAh/g at a C/10 rate (Figure 8 inset left) and 80% of the delivered capacity at a C discharge rate (Figure 8 inset right). This is a satisfactory result knowing that this sample was neither chemically coated nor ever treated at temperatures greater than

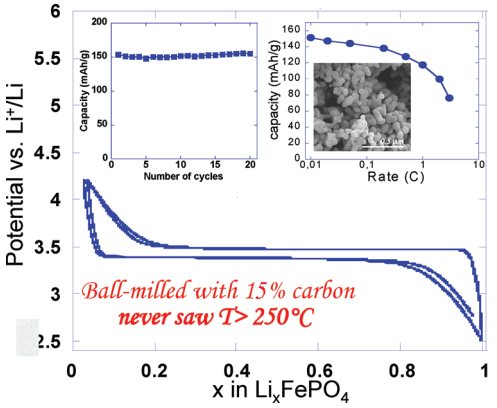

Figure 8. Voltage-composition profile together with the capacity retention (inset left) and power rate (inset right) for Li/$LiFePO_4$ half cells made using nanometric $LiFePO_4$ powders prepared in EMI-TFSI ionic liquid. The positive electrode, made by ball milling $LiFePO_4$ and carbon SP in a 85−15% weight ratio, contains 7.5 mg of active material per squared centimeter. A cycling rate of C/10 is used. Worth noting is that such an electrode never saw a temperature greater than 250 °C.

250 °C but simply ball-milled with 15% SP carbon for 15 min.

At this juncture, mindful of our success in the ionothermal synthesis of $LiFePO_4$ at temperatures below 250 °C, one may question its versatility and generalization to other known inorganic compounds. This synthetic approach was successfully applied to materials derived from the olivine-type structure ($LiMPO_4$ M = Mn, Co, and Ni),[16] as well as other electrode materials containing either (i) SiO_4 rather than PO_4 entities (Li_2FeSiO_4),[9] (ii) having F^- in addition to PO_4^{3-} as part of the anionic lattice [LiFe(Ti)PO_4F],[6] and (iii) Na^+ rather than Li^+ ions as guest cations ($Na_{2-x}Li_xFePO_4F$).[36] Experimental conditions together with structural information regarding the new phases reported herein are listed in Table 1. For reasons of conciseness, we will only focus on the synthesis of F-based compounds whose synthetic processes are not always straightforward and usually require, with a few exceptions, thermal treatment in sealed vessels or to be carried out under controlled environment to avoid

Table 1. List of All Compounds Discussed in the Paper Together with a Description of the Experimental Conditions (Heating Protocol) Enlisting the Nature of the Precursors and Ionic Liquids Used Together with Their Structural Information (Space Group)

Compound	Precursors	Ionic liquids	T(°C)	Time (h)	Particule size (nm)	Unit Cell/space group
$LiFePO_4$	LiH_2PO_4 $FeC_2O_4.2H_2O$	EMI-TFSI	250	24	150 - 300	*Pnma*
$LiMnPO_4$	LiH_2PO_4 $MnC_2O_4.2H_2O$	EMI-TFSI	250	24	100 - 400	*Pnma*
$LiMPO_4$ (M= Ni, Co)	LiH_2PO_4 $MC_2O_4.2H_2O$	EMI-TFSI	250	24	800 - 1000	*Pnma*
Na_2FePO_4F	Na_3PO_4 FeF_2/ $FeCl_2$	C2	270	48	< 50	*Pbcn*
Na_2MnPO_4F	Na_3PO_4 MnF_2/ $MnCl_2$	C2	270	48	< 50	$P2_1/n$
$Na_2Fe_{1-x}Mn_xPO_4F$ $0 \leq x \leq 0.15$	Na_3PO_4 MnF_2/ $MnCl_2$	C2	270	48	< 50	*Pbcn*
$Na_2Fe_{1-x}Mn_xPO_4F$ $0.25 \leq x \leq 1$	Na_3PO_4 MnF_2/ $MnCl_2$	C2	270	48	< 50	$P2_1/n$
$LiFePO_4F$	Li_3PO_4 FeF_3	Triflate	260	48	< 50	$P\bar{1}$
$LiTiPO_4F$	Li_3PO4 TiF_3	C2-OH	260	48	< 50	$P\bar{1}$
$LiFeSO_4F$	$FeSO_4.H_2O$ LiF	EMI-TFSI	280	48	600 - 1200	$P\bar{1}$
$LiMnSO_4F$	$MnSO_4.H_2O$ LiF	EMI-TFSI	280	24	600 - 1200	$P2_1/c$

EMI-TFSI	1-ethyl-3-methylimidazolium Bis(trifluoromethanesulfonyl)imide	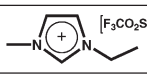
C2	1-butyl-2,3-dimethylimidazolium Bis(trifluoromethanesulfonyl)imide	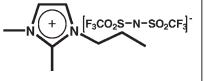
Triflate	1-butyl3-méthylimidazolium trifluorométhanesulfonate	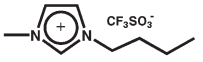
C2-OH	1,2-dimethyl-3-(3-hydroxypropyl)- imidazolium bis(trifluoromethane sulfonyl)imide	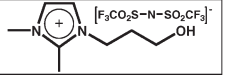

fluoride hydrolysis. Nevertheless, despite these identified difficulties, F-based compounds are regaining an increased interest as electrode materials because being capable of displaying greater potential than oxides electrodes. If not otherwise specified, the most classical, heavily used, and broadly commercialized EMI-TFSI ionic liquid, which is hydrophobic and thermally stable up to 290−300 °C, was always taken as the reacting medium in our attempt to implement ionothermal synthesis to the preparation of other inorganic compounds.

Ionothermal Synthesis of Na_2FePO_4F. Na_2FePO_4F crystallizes in an orthorhombic unit cell and adopts a two-dimensional structure in which the Na^+ ions are located between bidimensional layers composed of FeO_4F_2 octahedra and PO_4 tetrahedra. Nazar et al.[36] recently demonstrated Na_2FePO_4F, made via a ceramic process at temperature of 650 °C, to be an attractive intercalation compound with respect to both Na^+ and Li^+ guest ions. It was then tempting to test whether such a material, as well as the homologues Na_2MnPO_4F or Li_2FePO_4F, could be made more attractive for electrodes via ionothermal synthesis.

Our first attempts to prepare Na_2FePO_4F, in EMI-TFSI from Na_3PO_4 and MF_2, consistently failed regardless of the temperature used. This failure was ascribed to the deprotonation of the acidic C_2 hydrogen in the presence of basic species (F^-, PO_4^{3-}) and led us to use a C_2 protected 1,2-dimethyl-3-butylimidazolium bis-(trifluoromethanesulfonyl) imide ionic liquid. Na_2FePO_4F was then synthesized according to the following protocol: (i) under argon, in a 25 mL PTFE-lined steel bomb, 5 mL of DMBI-TFSI and stoichiometric amounts of M_3PO_4 and MF_2 (1:1) were combined, (ii) the bomb was then placed into an oven and the temperature was raised to 270 °C at a rate of 5 °C/min, and (iii) this temperature was maintained for 48 h. Once the oven had cooled down to room temperature, the powder and ionic liquid were separated by centrifugation, and the recovered powders were washed with cold water to remove most of the formed NaF phase. Under such conditions, single-phased and nanosized Na_2FePO_4F powders (Figure 9a), as deduced by complementary XRD and TEM measurements, were obtained (Table 1). Occasionally, the powders were contaminated with traces of NaF which cannot easily be washed away. An alternative to eschew the NaF residual issue consists of starting with equimolar mixtures of FeF_2 and $FeCl_2$ rather than FeF_2 alone, so that the reaction products turn out to be Na_2FePO_4F and NaCl, the latter being quite soluble in water or methanol.

Utilizing a similar heating protocol with the use of the same ionic liquid but with MnF_2 instead of FeF_2, we were able to synthesize the Na_2MnPO_4F phase which adopted a 3D rather than 2D structure. This structural difference results from the fact that the Mn phases, in contrast to the Fe one, share only one common F vertices and form $Mn_2F_2O_8$ chains parallel to the *b*-axis of the monoclinic unit cell (Figure 9b). These chains are linked in the *a* and *c* directions by a PO_4 tetrahedron leading to tunnels for possible cationic Na transport. We also used ionothermal synthesis as a high throughput synthetic method to rapidly map the $Na_2Fe_{1-x}Mn_xPO_4F$ phase diagram and determine that the 2D−3D structural transition did not occur at $x = 0.5$ but did occur at smaller Mn contents ($x = 0.2$). Finally, it is worth mentioning that this synthetic approach has its limitations as demonstrated by our failure to prepare Li_2FePO_4F by reacting FeF_2 with Li_3PO_4 or other precursors, most likely for thermodynamic reasons, as we constantly obtained mixtures of $LiFePO_4 + LiF$.

These ionothermally synthesized powders were found, like the bulk Na_2FePO_4F powders previously prepared via 700 °C ceramic process, to be electrochemically active. However, these new powders showed appreciably improved performances (Figure 9c) which were marked by a better initial capacity (120 mAh/g with $x \approx 1$), lower irreversible capacity, lower polarization, and better capacity retention over cycling. These improved performances can simply be ascribed to the nanosized character of our powders brought on by the ionothermal process. The superior performances of nanometric vs bulk electrodes were also confirmed for the first sodium Na_2FePO_4F/Na half cells. Conversely, and regardless of particle sizes, the pure Na_2MnPO_4F phase was found to be electrochemically inactive with respect to either Na or Li, and we observed that the inactivity was mainly triggered by the onset of the Mn-driven 2D−3D structural transition.[37]

Ionothermal Synthesis of Tavorite-type Phases $LiFePO_4F$ and $LiTiPO_4F$. As part of the resurgence of F-based electrodes, Barker et al.[38−41] have shown that $LiVPO_4F$, which is isostructural to Tavorite $LiFePO_4(OH)$,[42] can reversibly insert one Li at 4.1 V. On the basis of their findings, the authors synthesized, via a high temperature ceramic process enlisting several successive bake and shake steps, most of the 3d-metal lithium fluorophosphate $LiMPO_4F$ phases (M = 3d metal element) without reporting the electrochemical performances of the Fe and Ti members' despite their attractiveness costwise. We decided to follow this initial exploration[43] in an attempt to further demonstrate the versatility of ionothermal synthesis and the potential of $LiMPO_4F$ phases (M = Fe, Ti) as electrode materials for Li-ion batteries.

Prior to selecting our precursor materials, it was worth noting that our target compounds, as opposed to the other ones so far mentioned in this review, contained the 3d-metal in its (III) oxidation state. As ionic liquids are free of redox activity, this implies that we had to select $Fe^{(III)}$ and $Ti^{(III)}$ based precursors, and the first ones to come to mind both as sources of $Fe^{(III)}$ or $Ti^{(III)}$ and F^- are FeF_3 and TiF_3, respectively. Regarding the source of Li and phosphate, we stuck with Li_3PO_4 which had so far been successfully used in our previous syntheses.

At first, 5 mL of EMI-TFSI and stoichiometric amounts of FeF_3 and Li_3PO_4 (enough to prepare 1 g of $LiFePO_4F$) were combined and placed in a 25 mL

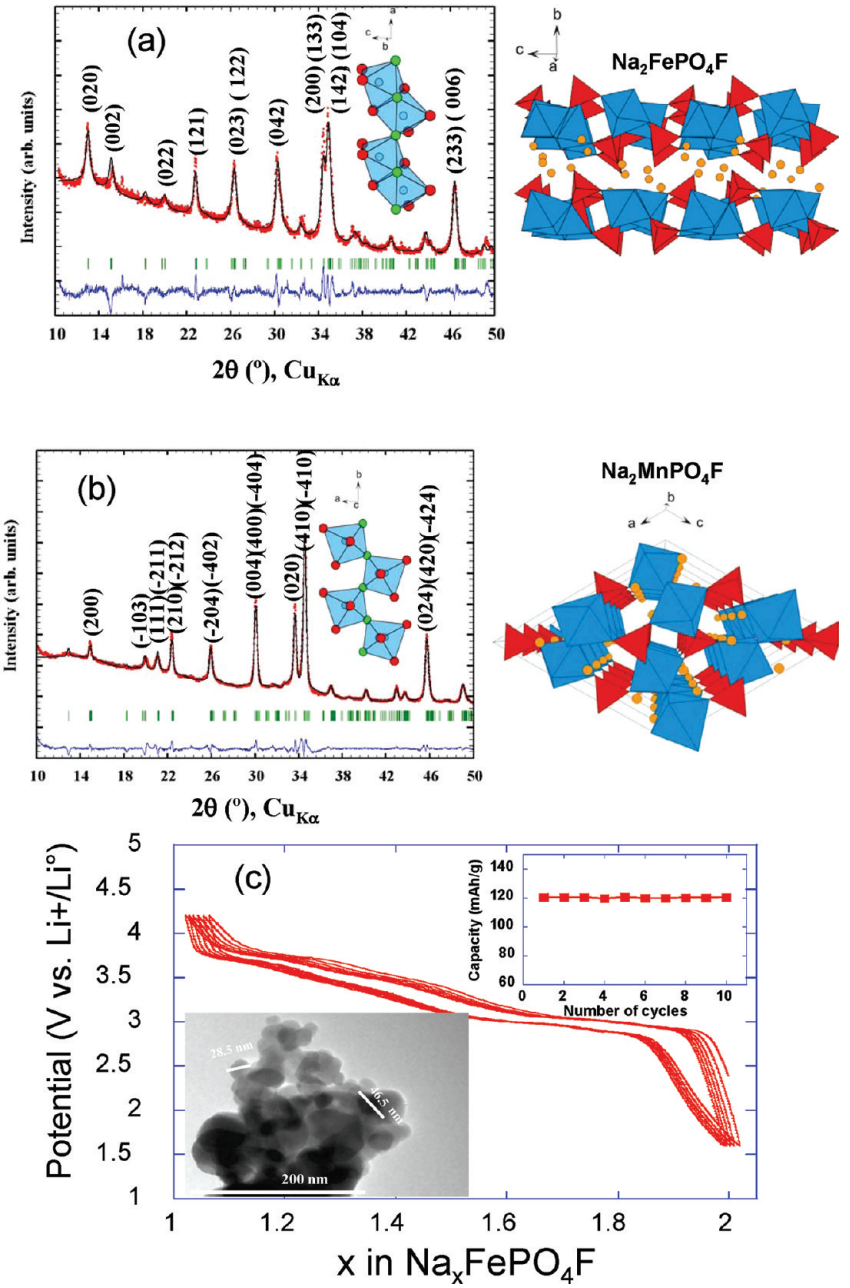

Figure 9. XRD diffraction patterns for the Na_2FePO_4F (a) and Na_2MnPO_4F (b) phases made in ionic liquid medium together with their corresponding 2D and 3D structures. Also highlighted is the packing of $Fe_2O_8F_2$ units (Na_2FePO_4F) and of MnO_4F_2 octahedra (Na_2MnPO_4F) which form chains running along the *b*-axis. The MO_4F_2 octahedra, PO_4 tetrahedra, and Na atoms are displayed in purple, green, and blue, respectively. In part c, the electrochemical characterization of Na_2FePO_4F samples vs Li via the ionothermal reaction using as precursor once NaF was removed by washing in cold water is shown together with a TEM picture of the nanopowders (left bottom inset) and the capacity retention upon cycling (right top inset). The samples were carbon-coated (5% in weight) using a 10 min sucrose pyrolysis treatment at 700 °C and then manually mixed with an additional 15% by weight of carbon SP. The electrode loading was 8.5 mg/cm^2, and a charge−discharge cycling rate of C/15 was used.

PTFE-lined steel bomb which was heated at temperatures ranging from 200 to 300 °C for about 48 h. No evidence of new phases was obtained until 260 °C, and surprisingly, for higher temperatures, we observed the formation of $LiFePO_4$ rather than $LiFePO_4F$ indicating the reduction of $Fe^{(III)}$ to $Fe^{(II)}$ in our reacting medium. On the basis of the distinct smell of H_2S when the bombs were opened, such a reduction was ascribed to the reactivity of $TFSI^-$ ions with FeF_3 to liberate sulfur. To alleviate this issue, we replaced the $TFSI^-$ anion by a trifluoromethanesulfonate (triflate) one, which was found to be stable with respect to FeF_3. Next using 1-butyl-3-methylimidazolium triflate as the reacting media and a temperature of 260 °C for 48 h, we succeeded in preparing single-phased and nano-metric $LiFePO_4F$ powders as deduced by XRD and TEM measurements, respectively (Figure 10a).

In regard to the synthesis of $LiTiPO_4F$, it should be recognized that $Ti^{(III)}$ ions are more stable than $Fe^{(III)}$ ions so the use of triflate anions is no longer necessary. However, due to this enhanced stability, higher reaction temperatures were necessary since no sign of reaction was observed when stoichiometric amounts of TiF_3 and

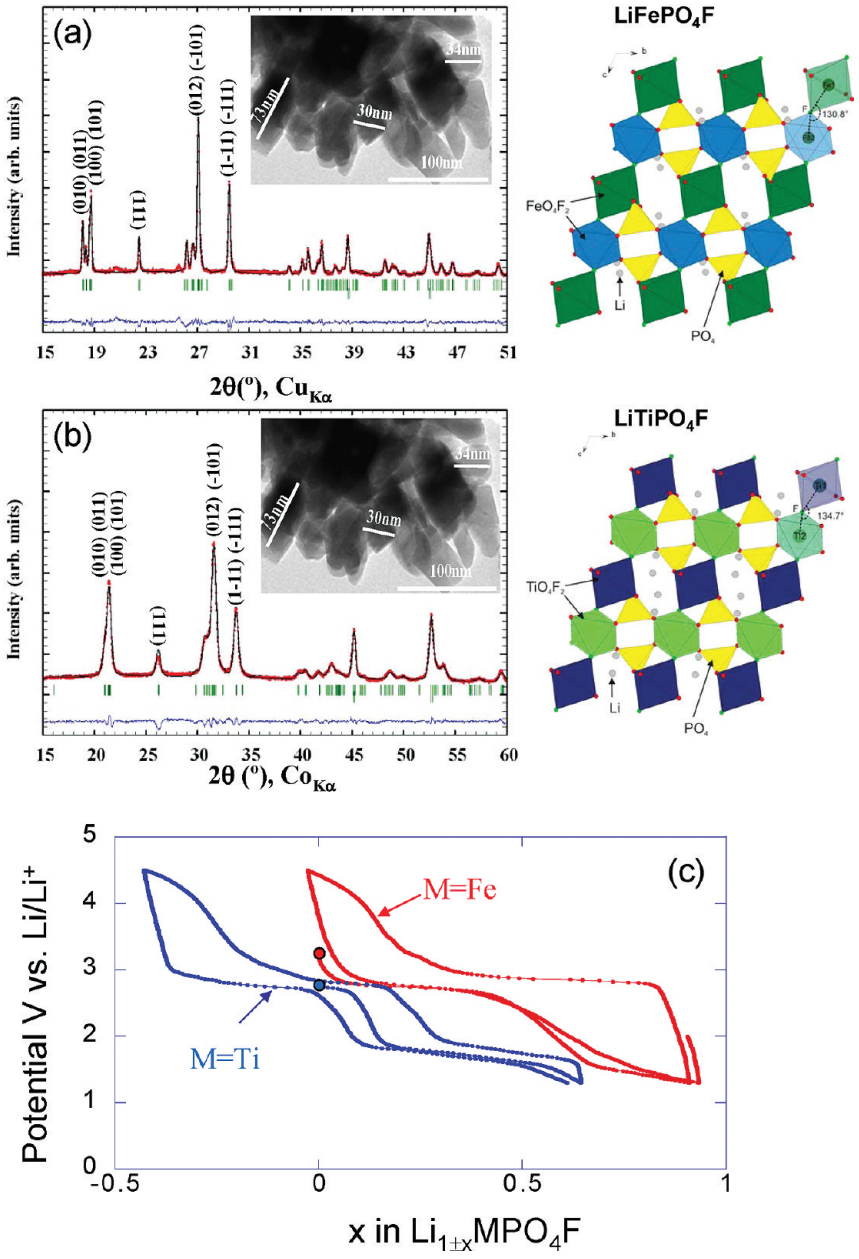

Figure 10. XRD powder patterns for the $LiFePO_4F$ (a) and $LiTiPO_4F$ (b) phases ionothermally prepared together with their corresponding morphology as deduced by SEM and structural projection along the *c*-axis. Note the M_1-F-M_2 angle difference between the two structures. The voltage−composition curves obtained from cycling Li/$LiFePO_4F$ and Li/$LiTiPO_4F$ cells are shown in part c. The cells were cycled at a C/15 rate. The electrodes, whose active weight was 6 mg ($LiFePO_4F$) and 7.9 mg ($LiTiPO_4F$), were made by ball milling for 15 min the active material and carbon SP in a 85−15% weight ratio.

Li_3PO_4, dispersed in 5 mL of EMI-TFSI, were heated to 270 °C for 48 h. Additionally, longer reaction times led to a severe darkening of the ionic liquid while only traces of the proper $LiTiPO_4F$ phase were detected suggesting that this reaction is kinetically limited. To eschew both of the above issues, namely darkening of the ionic liquid and low reactivity, we first substituted the C_2 acidic proton for a methyl group to limit its possible attack by TiF_3 and thus the electrolyte degradation, and second, we functionalized the alkyl chain with an OH group so as to reduce the reaction temperature via increasing the precursors solubility. Using the in-house 1,2-dimethyl-3-(3-hydroxypropyl)-imidazolium bis(trifluoromethane sulfonyl)-imide ionic liquid, we could then obtain, after 48 h of heating at 260 °C, single-phased and nanosized $LiTiPO_4F$ powders (Figure 10b). Both $LiFePO_4F$ and $LiTiPO_4F$ are isostructural to Tavorite $LiFePO_4(OH)$ and crystallize in a triclinic cell (space group $P\bar{1}$), with lattice parameters reported in Table 1. Basically, their structure consists of metal centered octahedra MO_4F_2 (M = Fe, Ti) linked together by fluorine vertices in trans position forming chains along the *c*-axis.

For comparison, 700 °C is the minimum temperature required to make micrometer-sized $LiFePO_4F$ or $LiTiPO_4F$ powders by solid-state reactions from the same (MF_3 + Li_3PO_4) precursors. Moreover, owing to the moisture sensitivity of the 3d-metal fluoride precursors, these reactions must be conducted in sealed platinum (Fe) and stainless steel (Ti) vessels. This once again illustrates the many benefits attributed to the ionothermal synthesis

for inorganic materials once the proper ionic liquid has been identified.

Figure 10c shows the electrochemical performances of the $LiFePO_4F$ and $LiTiPO_4F$ electrodes (made by ball-milling $LiMPO_4F$ with 15% SP carbons for 15 min) vs Li. Both compounds show, over the 1.2−4.5 V voltage range, a reversible electrochemical activity of nearly one lithium per unit formula and a polarization at least twice smaller than that measured for micrometric powders. Another key feature present in both compounds but more pronounced in $LiTiPO_4F$ is the staircase variation of the voltage with composition, with two pseudo-plateaus of equal amplitude (0.5 Li^+) corresponding most likely to the oxidation of $Ti^{(III)}$ into $Ti^{(IV)}$ (2.9 V) and the reduction of $Ti^{(III)}$ into $Ti^{(II)}$ (1.7 V). This is similar to what was reported for $LiVPO_4F$,[43,44] with the difference being that the two plateaus were located at 4 and 3 V with each having a capacity of one Li. $LiFePO_4F$, which also shows a slight staircase voltage variation when discharged, which then disappears upon charging. It can uptake one Li leading to the Li_2FePO_4F phase, also having a Tavorite-type structure. Such subtleties, namely the limitation of the $Ti^{(III)}$ oxidation or reduction to 0.5 $Ti^{(IV)}$ or 0.5 $Ti^{(II)}$, and different charge/discharge profiles are rooted in structural considerations which fall beyond the scope of this paper.

Hunting for Novel Materials. All the specific aforementioned examples have illustrated the positive attributes of ionothermal synthesis in elaborating known electrode materials with tailored size and morphology. However, for a novel synthetic approach to reach common acceptance in the scientific community, it has to enable groundbreaking material discoveries. The design of new materials and structures that provide high energy densities, long cycle life, and high power rates is crucial to the development of battery technologies. Although high throughput computational searches can provide guidance for new structures to maximize energy density and Li-ion mobility, it remains the job of the chemist, with his/her intuition and modest toolkit consisting of structural, electronegativity, ionocovalency, and thermodynamic considerations together with his/her ability to employ phase homologies, to come up with the new phases, as will be shown below.

Simple ionocovalency can directly be used to explain why sulphide-based compounds, which are more covalent than oxides, have a lower intercalation voltage. Such a concept was even beautifully generalized by Goodenough[43−45] and termed the "inductive effect" to predict, among isostructural polyanionic compounds, relative voltage changes triggered by various polyanion substitutions. Consistent with the larger electronegativity of sulfur vs phosphorus, it has been shown that substituting phosphate $(PO_4)^{3-}$ for sulfate $(SO_4)^{2-}$ anions in an isostructural NASICON $Li_xM_3(XO_4)_3$ increases the open-circuit voltage by 0.8 V, regardless of the 3d-metal considered.[45] Within this context, our work on the fluorophosphates $Li(M)PO_4F$ (M = Ti, Fe), despite not leading to a potentially interesting electrode material because their redox potential of 2.8 V is to low, turned out to be quite relevant. Indeed, such materials belong to the vast Tavorite family among which one other Fe-based material ($LiFePO_4(OH)$)[46] has been reported to reversibly intercalate Li at 2.6 V; 0.2 V lower than that of $LiFePO_4F$,[37] which is consistent with the greater electronegativity of F^- as compared to OH^-. Along that line, one could simply predict, using simple addition, that if we could maintain the Tavorite-type structure and replace all the $(PO_4)^{3-}$ with $(SO_4)^{2-}$ anions, we would see a 0.8 V potential increase. Therefore, by pursuing the phase homology concept, which can forecast specific new phases with high probability, we can conclude that the $LiFeSO_4F$ Tavorite phase should exist, and it should display a redox potential of 3.6 V. Although research on that topic has been hardly prolific over the last decades, as only one fluoro-sulfate phase ($LiMgSO_4F$) having the Tavorite structure was ever reported in the literature by Piffard et al.,[47] we decided to further explore the fluorosulfate chemistry.

Owing to our success in synthesizing $LiFePO_4F$ by ionothermal synthesis at 260 °C, we decided to apply this approach to the synthesis of $LiFeSO_4F$[48] in an attempt to stabilize product formation. When deciding between the two main possibilities for reactants, (FeF_2 + Li_2SO_4) or ($FeSO_4 \cdot nH_2O$ + LiF) in EMI-TFSI, we chose the latter noting the advent of a new phase in our resulting products only when the iron sulfate phase contained water. Such an observation led us to contemplate the crystal structure of several iron sulfate hydrate phases (n = 7, 4, and 1), and among them $FeSO_4 \cdot H_2O$, which adopts the Szomolnokite-type structure,[48] appears most closely related to that of the tavorite $LiMgSO_4F$ phase.[49] Indeed, by comparing the fluoro-sulfate structure projected along the [100] direction to that of the monohydrated sulfate one along [$\bar{1}$10] direction, it appeared like they were displaying the same sequence of octahedral and tetrahedral sites. The oxygen site corresponding to the H_2O molecule in $FeSO_4 \cdot H_2O$ is also interesting because it is identical to the fluorine site in the $LiMgSO_4F$ structure, which could lead to the possibility of double Li^+ for H^+ and F^- for OH^- ion exchange reactions.

Guided by this structural relation, $FeSO_4 \cdot H_2O$ was selected as our precursor phase.[50] Typical experiments were then conducted in a 25 mL PTFE-lined steel bomb by reacting at 275 °C for 24 h equimolar amounts of $FeSO_4 \cdot H_2O$ and LiF dispersed into 5 mL of EMI-TFSI. Under such conditions single-phased $LiFeSO_4F$ was synthesized for the first time. As expected from our line of reasoning based on phase homology, $LiFeSO_4F$ adopts the Tavorite-type structure (space group $P\bar{1}$) with lattice constants: a = 5.1747(3) (Å), b = 5.4943(3) (Å), c = 7.2224(3) (Å), α = 106.522(3), β = 107.210(3), γ = 97.791(3), and V = 182.559(16) (Å^3) (Figure 11), with channels running along the [**100**], [**010**], [**001**] and [**111**] direction for Li-ions to migrate. Additionally, we found that high purity $LiFeSO_4F$ can be synthesized in covered PTFE containers containing the same reaction mixture as above, but heated to 300 °C over 4 h and maintained at

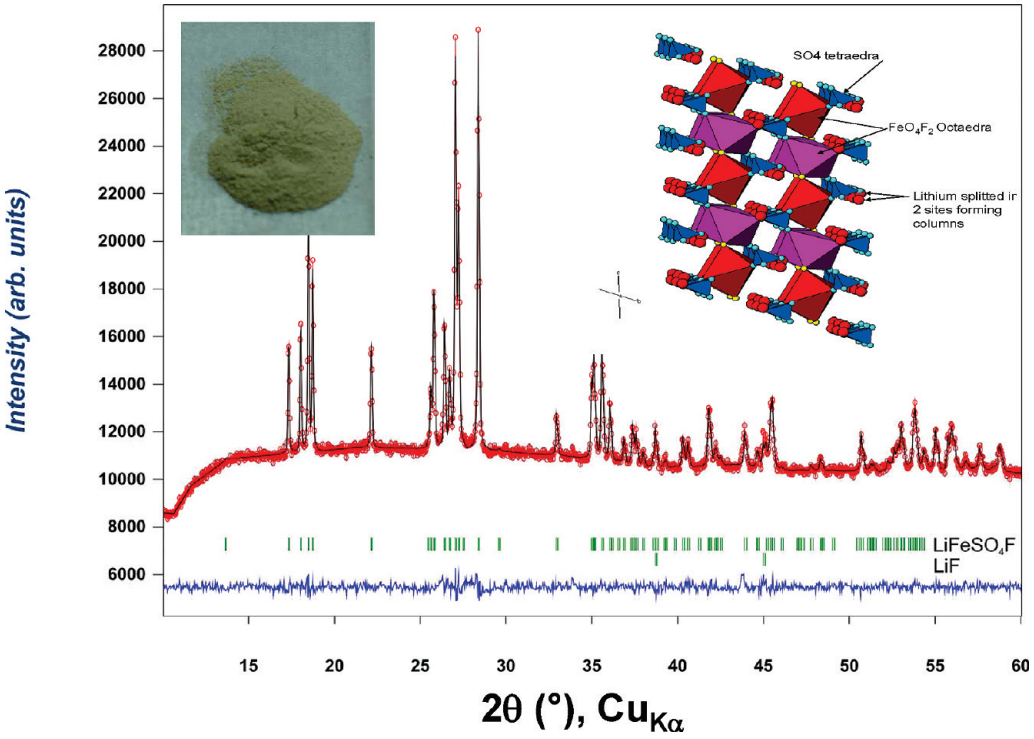

Figure 11. X-ray powder pattern of $LiFeSO_4F$ together with as inset its corresponding structure deduced from Rietveld refinement. Note the two crystallographically independent and slightly distorted iron-based FeO_4F_2 octahedra (red and purple) linked together by fluorine vertices (yellow) in the *trans* position forming chains along the *c*-axis which are bridged together by isolated SO_4 tetrahedra (blue) creating a tunnel within which the Li-ions (red) are nested. The color-like appearance of $LiFeSO_4F$ powders is shown as well as inset.

this temperature for an additional 4 h. This method both shortens the reaction time and eliminates the use of cumbersome steel bombs.

To further confirm the importance of the structural relationship between the precursor and the end phase previously spotted in ruling the double exchange reaction, we reacted other 3d-metal $MSO_4 \cdot H_2O$ phases such as $MnSO_4 \cdot H_2O$, $CoSO_4 \cdot H_2O$, and $NiSO_4 \cdot H_2O$ (isostructural to $FeSO_4 \cdot H_2O$) with LiF in EMI-TFSI. We succeeded in preparing the corresponding fluorosulfates $LiMSO_4F$ (M = Mn, Co, and Ni) at temperatures lower than 310 °C never reported until now. Two of these new materials (Co and Ni) crystallize in the same unit cell-type as $LiFeSO_4F$ (e.g., triclinic $P\bar{1}$), while $LiMnSO_4F$ crystallizes in a monoclinic unit-cell space group ($P21/c$) (Table 1). With the exception of Mn, the new phases[50] are metastable and all decompose at temperatures beyond 375 °C, explaining why they could not be isolated via a ceramic approach. Additionally, $LiFeSO_4F$ decomposes in water which explains why it could not be previously synthesized via low temperature solution chemistry in aqueous media. It is worth mentioning that, among the "d-metal based fluorosulphate phases", the Fe-based phase is one of the trickiest to make, because it is difficult to keep the monohydrated precursor free of $Fe^{(III)}$. Moreover, neither of these reactions could proceed by pressing all the components into a pellet and heating them to 300°C under argon for times ranging from 2 to 10 h, which indirectly indicated that the ionic liquid is active in the growing process of the newly born phases. Most likely, the solid-state synthesis needs longer annealing duration to yield the desired product phases.

The ionothermal growth of $LiFePO_4$ has previously been shown to proceed via solution-based reactions; however, the precursors $FeC_2O_4 \cdot 2H_2O$ and LiH_2PO_4 were poorly soluble in the solvents that were used. It was determined that $FeSO_4 \cdot H_2O$ is not soluble in EMI-TFSI because mixtures of $FeSO_4 \cdot H_2O$ + EMI-TFSI at 300 °C resulted in the formation of $FeSO_4$. In contrast, LiF is sparingly soluble (2 g/L) at elevated temperatures, which we demonstrated by bringing LiF + EMI-TFSI to 290 °C and withdrawing aliquots of ionic liquids out of which we could precipitate tiny amounts of LiF. Though minuscule, this solubility of LiF helps the double exchange reaction to proceed. Therefore, our observation of the 50 °C temperature difference of the iron monohydrate phase depending upon whether it is annealed in the presence of ionic liquids (270 °C) or free of ionic liquid (220 °C), as deduced by DSC (Figure 12), indicates that the ionic liquid introduces a kinetic lag in the removal of water, which we believe to be crucial for the reaction to proceed properly. The ionic liquid can be viewed as an encapsulating medium[48] which delays the water release from the monohydrated phase and, therefore, gives enough time to the ion exchange to proceed. Our observations of the inability to prepare $LiFeSO_4F$ by rapidly raising the temperature of our reaction ($FeSO_4 \cdot H_2O$ + LiF + EMI-TFSI) mixture to 300 °C (e.g., removing water prior to triggering the ion exchange) or by using microwave-assisted heating support the correctness of our reaction scheme. Therefore, its full role is provided

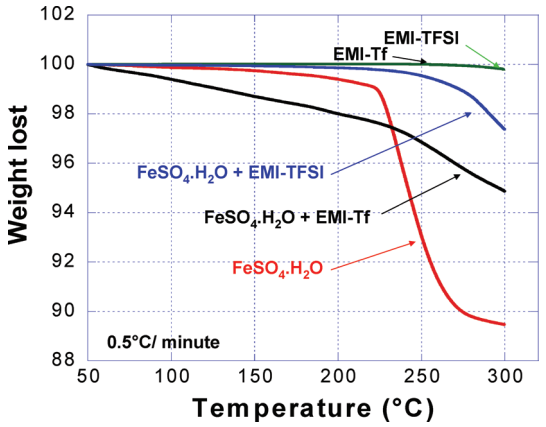

Figure 12. Variation of the weight loss as a function of temperature for $FeSO_4 \cdot H_2O$, EMI-TFSI, and EMI-Tf samples and $FeSO_4 \cdot H_2O$−EMI-TFSI and $FeSO_4 \cdot H_2O$−EMI-Tf samples. Note the kinetic water lag introduced by the presence of the hydrophobic ionic liquid (EMI-TFSI) as compared to the hydrophilic one (EMI-Tf). The experiments were conducted in air at a heating rate of 1 °C/min.

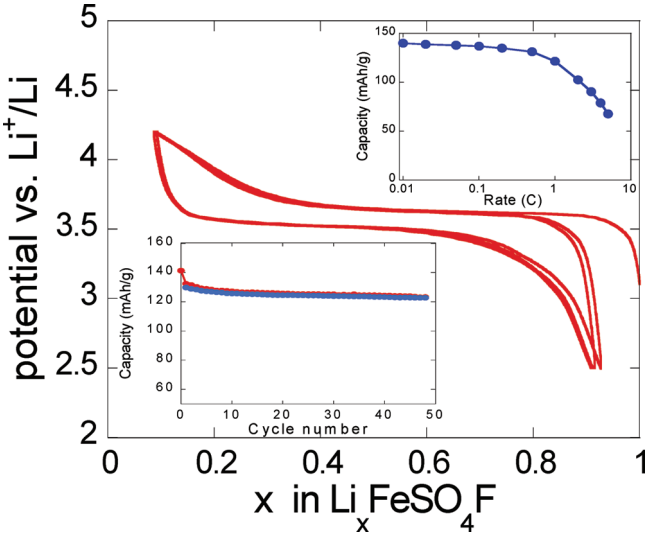

Figure 13. Charge/discharge galvanostatic curves for a Li/$LiFeSO_4F$ cell, which was cycled at a rate of C/10, together with its capacity retention (inset lower left corner). Also shown (inset top right corner) is the power rate of $LiFeSO_4F$/cells as determined by the collection of signature curves using a cutoff discharge voltage of 2.5 V. The positive electrodes were prepared by ball-milling $LiFeSO_4F$ and carbon SP in a 85−15% weight ratio. Loading of 7−9 mg of active material per squared centimeter was used.

by the difficulties encountered in making $LiFeSO_4F$ with ionic liquids that are less hydrophobic than EMI-TFSI such as EMI-Tf (e.g., which will be a less efficient barrier toward water release).

Among all the newly synthesized phases, only $LiFeSO_4F$ shows attractive electrochemical performance (Figure 13). The voltage−composition trace for a Li/$LiFeSO_4F$ cell cycled between 4.2 and 2.5 V at a C/10 rate (1 Li in 10 h) shows an electrochemical activity, centered around 3.6 V, involving the reversible uptake and release of 0.85 Li^+ ions leading to a practical density of about 130 to 140 mAh/g of $LiFeSO_4F$. Without a doubt, further electrode optimization will bring this capacity closer to the theoretical value of 151 mAh/g. Additionally, the small difference between the charge and discharge curves is characteristic of good electrode kinetics and is confirmed by power rate capability tests (Figure 13 top inset). Overall, the electrochemical performances of $LiFeSO_4F$, although this material was discovered only a few months ago, are benchmarking close to those of $LiFePO_4$, which has been studied worldwide for the past decade. Finally, it is both amusing and vexing that our inelegant back-of-the-envelope method of anticipating a redox activity value for a compound based on simple chemical concepts turned out to be quite accurate. Maybe there is a lesson on designing new electrode materials to be learned from.

Conclusions/Outlook and Perspectives

Historically, the performances of electrodes have been benchmarked in terms of capacity, energy density, and power rate with the life cycle cost only being considered as a plus. However, in order to make emerging $LiFePO_4$/C Li-ion battery technology a viable option for tomorrow's EVs and HEVs, low temperature eco-efficient electrode processes must be developed. Clearly, without this present energy-related drive, the field of energy storage and, more so, of inorganic synthesis would not have enjoyed such a prolific time. We have shown enormous progresses toward the elaboration of synthetic $LiFePO_4$ via cleverly adapted and modified hydro- and solvothermal processes including (i) the addition of high boiling solvents such as DMSO to enable precipitation at high temperatures, (ii) the use of latent bases as a means to alleviate the formation of $Fe^{(III)}$, which is always a nightmare when preparing $Fe^{(II)}$-based compounds at low temperatures while saving expensive Li sources, and (iii) the possibility of assisting all of these processes by microwave heating to shorten preparation time. For each process, the nature of the precursors was adapted not only to tailor the morphology and size of the resulting particles with the help of surfactants but also to make sure that the reaction could proceed both with an economy of atoms and the formation of easily disposable side products. Water-based synthesis processes enlisting the use of autoclaves are easily scalable to tonnes of production in industry with therefore increased safety requirements when temperatures greater than 180 °C must be used. Laboratory autoclaves on the other hand are, due to their small size, safe beyond rated temperature and pressure but cannot be left in the hand of uninformed personnel.

With the initial driving force toward the production of chemically stable olivine by a green chemistry route, we introduced ionothermal synthesis to the field of inorganic synthesis. Using various ionic liquids as reaction media, phase-pure $LiFePO_4$ with tunable morphology and crystallographic orientations were obtained. Inspired by this finding, we have successfully generalized this synthetic approach to other known electrode materials that we recently made via this technique. Bearing in mind that ionic liquids are room temperature molten salts, and that molten salts have long been used in inorganic synthesis, this recent development may appear trivial to some.

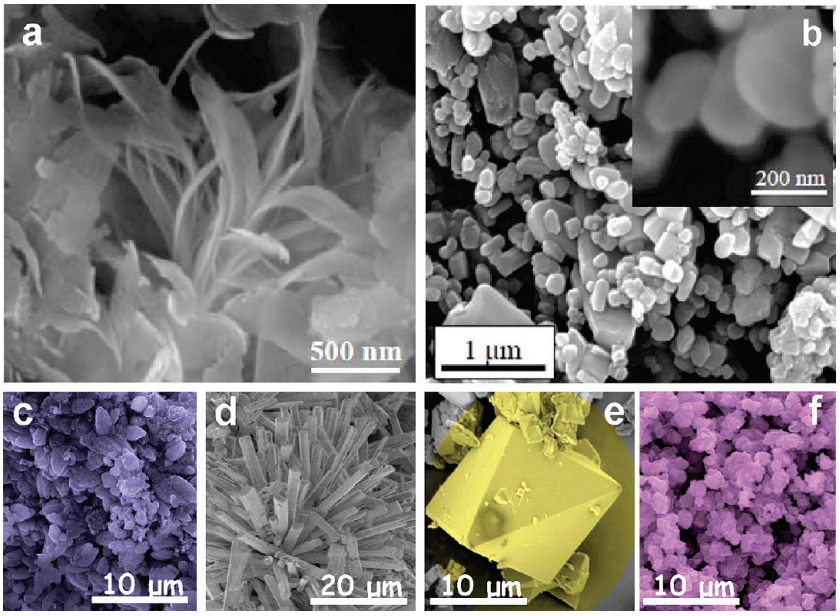

Figure 14. (a) Modified ionothermal synthesis of $LiMnPO_4$ using a mixture of EMI-TFSI and diethylene glycol as the reacting medium giving rise to platelet morphology. (b) Addition of water along with surfactant creating small water droplets inside the ionic liquid, which acts as a nanoreactor developing nanostructured, phase-pure $LiMnPO_4$ with spherical morphology. (c−f) SEM images of phase-pure $LiMnPO_4$ produced by varied combination of ionic liquids and precursors giving rise to diverse morphology.

However, this is without considering that previous molten salt approaches usually called for high temperatures and non trivial recovery of the materials from the fluxes, often requiring melt centrifugation or chemical etching, with the inherent risk of non chemical stability between the etchant and the prepared material. On the other side, molten salts are inexpensive fluxes while ionic liquids are costly if used once per reaction. However, we have shown that they can be continuously reused in industrial type preparation without purification when used to prepare the same material.[16] To support this statement, the NMR spectra of a fresh EMI-TFSI sample and an EMI-TFSI, which has been recuperated from the synthesis of $LiFeSO_4F$ at 280 °C, are identical. Presently, the most expensive part of the ILs used herein is the anion $TFSI^-$ (at 200 €/kg) when sold in small volumes, which can then be assumed to be an upper estimate of the IL price. With 99% recovery (including concentrating the rinsing with volatile organic solvents like acetone) and 200 g of ceramic/L of IL per batch, the lost IL would account to 10 €/kg at most to be compared with electrode materials in the 30−60 €/kg.

Although ionothermal synthesis cannot be used blindly, we have shown throughout this review that there are many choices available, owing to the large number of cations and anions, to design the proper ionic liquid with the right polarity, hydrophobicity, solvating properties, and thermal stability to not only trigger the growth of a specific compound, but also adjust its morphology/particle size. Therefore, much more remains to be done, for instance (i) investigating the effect of linear vs branched ionic liquids on particle morphology, (ii) using an ionic liquid not only as a reacting medium to orient crystal growth direction but to also stabilize polymorphs in polymorph-rich systems such as Li_2FeSiO_4 (α, β, and γ). Additionally, ionic liquids offer numerous opportunities, not yet fully explored, when used with other reaction solvents (diols or water). Diols are widely used in solvothermal synthesis acting as chelating agents and controlling the particle growth and morphology. When diols are added to ionic liquids (e.g., EMI-TFSI), they form a homogeneous mixture, stable up to the decomposition temperature of ionic liquids. This modified reactive medium reduces the synthesis temperature by at least 50 °C and facilitates single-phased product formation. Further, the addition of diols into ionic liquids develops a platelet-shaped morphology as shown in Figure 14a, which can affect the final electrochemical performance of electrode materials. In addition to diols, ionothermal synthesis can be modified by addition of water. Although ionic liquids are mostly hydrophobic in nature, small water droplets can be formed inside ionic liquid media with the help of surfactants. These surfactant-clad water droplets form a well-dispersed group of fine water micelles inside the ionic liquid. During reaction, the water micelles uptake the precursors due to higher solubility and carry the reaction forward, acting as a "nanoreactor" facilitating the formulation of nanoscale materials. The proof-of-concept work has been performed in the case of $LiMnPO_4$ olivine electrodes, which yield single-phased, nanostructured products with near spherical powder morphology (Figure 14b). The usage of different types of ionic liquids and precursors can lead to diverse morphology and structural variation as shown with some selected $LiMnPO_4$ products in Figure 14c−f. We are successfully carrying out various modified ionothermal syntheses of olivine $LiMnPO_4$, which will be shortly reported elsewhere.[51]

In addition to tuning the morphology of known materials to nanoscale dimensions and dramatically lowering

synthetic temperatures with respect to ceramic processes, ionothermal synthesis has enabled the synthesis of new fluorophosphate/fluorosulphate phases. Such a finding is important to both applications (as $LiFeSO_4F$ stands as a serious contender to $LiFePO_4$ for EV applications) and fundamental studies alike. This discovery opens the door to a totally new family of compounds which are attractive to both the field of electrode materials and the field of memory storage as some of them present peculiar magnetic properties to be reported in a forthcoming paper. Having shown the existence of new phases, we can now, based on the phase homology approach, speculate about the existence of other metastable fluorosulphates having the tavorite or derived structures. Last but not least, ionothermal synthesis can also be used as a high throughput method to rapidly scan phase diagrams because it can proceed in normal glassware and speed up by microwave-assisted heating. Microwave reactions are now well-documented in preparative organic chemistry, and a new equipment controls temperature and energy fluxes efficiently. We have in some cases experienced runaway reactions with ILs in microwave ovens, which may be linked to the very high conductivity of the ionic liquid especially at high temperatures, and this probably calls for a different approach to power regulation.

As with every new synthetic process, ionothermal synthesis comes with its own mysteries, and at the present stage, we realize that our understanding of the process is still very sketchy owing to difficulties in setting the proper in situ experiments to track reaction paths. Thermogravimetric analysis (TGA) measurements have been quite useful in showing that (1) $LiFePO_4$ only occurs once the decomposition of the precursor has started suggesting a solution growth/nucleation process; however, the nature of the decomposition-driven soluble released species escapes detection; and (2) ionic liquids can introduce kinetic lags in material dehydration ($FeSO_4 \cdot H_2O \rightarrow FeSO_4$). Therefore, we must place a greater effort into determining the solubility temperature dependence of the precursors we are using. Our attempts to direct crystal growth direction with ILs have so far remained very empirical as well since they mainly rely on trial approaches. Materials surfaces and interfaces between materials and ionic liquids obviously play a major role, and major efforts must be devoted to surface energy calculations; this could provide an invaluable insight into how we can better use ionic liquids to tailor the morphology of materials on demand.

Although, a broad development of ionothermal-driven inorganic synthesis is expected over the coming years, we should not neglect the resurgent interest for biomineralization synthetic approaches. For more than millions of years micro-organisms have learned how to make nanostructured materials or hierarchical porous structures under ambient conditions. Biologically induced mineralization via the use of a bacterium by the name "*Bacillus pasteurii*" has long been reported for calcite precipitation. Using the same bacterium to provoke the hydrolysis of urea and generate a basic medium, we recently witnessed some evidence of the possible growth of $LiFePO_4$ nanofilaments at temperatures as low as 65 °C, although reproducibility still remains an issue not yet mastered. Further supporting this trend toward biomimetic approaches is Belcher's recent work[52,53] on the use of engineered viruses as templates to make, at room temperature, high rate $FePO_4$/single-walled carbon nanotubes electrodes. Owing to the growing importance of materials sustainability and renewability for the years to come, biological principles will become more intensely implemented in the rational design and assembly of battery components.

Overall, the stringent properties required to produce low cost and highly performing electrode materials for Li-ion batteries have challenged our solid-state chemistry community for more than 25 years. Challenges call for progress and the need to turn insulating $LiFePO_4$ into an attractive electrode material is certainly no exception. A diverse array of innovative and diversified synthesis approaches, requiring cooperative efforts between inorganic, organic, and biochemists, have been developed leading to important advances in tuning existing materials and in designing novel electrode materials. Owing to chemistry, the future for Li-ion batteries looks bright indeed.

Acknowledgment. The authors would like to thank all the members of the LRCS M. Courty, C. Masquelier, C. Delacourt, and K. Djellab as well as members of the ALISTORE-ERI nanopositive team for fruitful discussions. The authors thank Ms. Michéle Nelson for proof-reading and improving the semantic aspects of the article.

References

(1) Kates, R. W.; Clark, W. C.; Correll, R.; Hall, J. M.; Jaeger, C. C.; Lowe, I.; et al. *Science* **2001**, *292*, 641–642.
(2) Armaroli, N.; Balzani, V. *Angew. Chem., Int. Ed.* **2007**, *46*, 52–66.
(3) Nagaura, T. K. *Progr. Batteries Solar Cells* **1990**, *9*, 209.
(4) Tarascon, J.-M.; Armand, M. *Nature* **2001**, *414*, 359–367.
(5) Rouxel, J.; Danot, M.; Bichon, J. *Bull. Soc. Chim.* **1971**, *11*, 3930–3936.
(6) DiSalvo, F. J.; Schwall, R.; Geballe, T. H.; Gamble, F. R.; Osiecki, J. H. *Phys. Rev. Lett.* **1971**, *27*, 310–313.
(7) Steele, B. C. H. Chemical Diffusion. *Fast Ion Transport in Solids*; Van Gool, W., Ed.; North Holland: Amsterdam, 1973; pp 103−109.
(8) Padhi, A. K.; Nanjundaswamy, K. S.; Goodenough, J. B. *J. Electrochem. Soc.* **1997**, *144*, 1188–1194.
(9) Nytén, A.; Abouimrane, A.; Armand, M.; Gustafsson, T.; Thomas, J. O. *Electrochem. Commun.* **2005**, *7*, 156–160.
(10) Abouimrane, A.; Armand, M.; Ravet, N. Carbon nano-painting: Application to non-phosphate oxyanions, e.g. Borates, Extended abstract. *203rd Meeting of the Electrochemical Society*, Paris, April 27−May 2, **2003**.
(11) Poizot, P.; Laruelle, S.; Grugeon, S.; Dupont, L.; Tarascon, J.-M. *Nature* **2000**, *407*, 496–499.
(12) Kepler, K. D.; Vaughley, J. T.; Thackeray, M. M. *Electrochem. Solid-State Lett.* **1999**, *2*, 307–309.
(13) Chen, J.; Wang, S.; Whittingham, M. S. *J. Power Sources* **2007**, *174*, 442–448.
(14) Delacourt, C.; Poizot, P.; Levasseur, S.; Masquelier, C. *Electrochem. Solid-State Lett.* **2006**, *9*, A352–A355.
(15) Recham, N.; Armand, M.; Laffont, L.; Tarascon, J.-M. *Electrochem. Solid-State Lett.* **2009**, *12*, A39–A44.
(16) Recham, N.; Dupont, L.; Courty, M.; Djellab, K.; Larcher, D.; Armand, M.; Tarascon, J.-M. *Chem. Mater.* **2009**, *21*, 1096–1107.
(17) Arico, A. S.; Bruce, P.; Scrosati, B.; Tarascon, J.-M.; Van Schalkwijk, W. *Nat. Mater.* **2005**, *4*, 366–377.
(18) Taberna, L.; Mitra, S.; Poizot, P.; Simon, P.; Tarascon, J.-M. *Nat. Mater.* **2006**, *5*, 567–573.
(19) Armand, M.; Tarascon, J.-M. *Nature* **2008**, *451*, 652–657.
(20) Livage, J. *Mater. Sci. Forum.* **1994**, *152−153*, 43–54.

(21) Ravet, N.; Goodenough, J. B.; Besner, S.; Simoneau, M.; Hovington, P.; Armand, M. Improved iron based cathode materials. *ECS Fall meeting*, Hawaii, October 17−22, **1999**; abstract no. 127.
(22) Ostwald, W. Z. *Z. Phys. Chem.* **1901**, *37*, 385.
(23) Yang, S.; Zavalij, P. Y.; Whittingham, M. S. *Electrochem. Commun.* **2001**, *3*, 505–508.
(24) Springsteen, L. L.; Matijevic, E. *Colloid Polym. Sci.* **1989**, *267*, 1007–1015.
(25) Wang, L. F.; Sondi, I.; Matijevic, E. *J. Colloid Interface Sci.* **1999**, *218*, 545–553.
(26) Sondi, I.; Matijevic, E. *J. Colloid Interface Sci.* **2001**, *238*, 208–214.
(27) Muraliganth, T.; Murugan, A. V.; Manthiram, A. *J. Mater. Chem.* **2008**, *18*, 5661–5668.
(28) Bilecka, I.; Hintennach, A.; Djerdj, I.; Novak, P.; Niederberger, M. *J. Mater. Chem.* **2009**, *19*, 5125–5128.
(29) Ueki, T.; Watanabe, M. *Macromolecules* **2008**, *41*, 3739–3749.
(30) Wasserscheid, P.; Welton, T. *Ionic Liquids in Synthesis*; Wiley-VCH: Weinheim, 2003.
(31) Armand, M.; Endres, F.; Macfarlane, D. R.; Ohno, H.; Scrosati, B. *Nat. Mater.* **2009**, *8*, 621–629.
(32) Parnham, E. R.; Morris, R. E. *Acc. Chem. Res.* **2007**, *40*, 1005–1013.
(33) Lin, Z. J.; Li, Y.; Slawin, A. M. Z.; Morris, R. E. *Dalton Trans.* **2008**, *30*, 3989–3994.
(34) Morris, R. E. *Chem. Commun.* **2009**, *21*, 2990–2998.
(35) Papaiconomou, N.; Yakelis, N.; Salminen, J.; Bergman, R.; Prausnitz, J. M. *J. Chem. Eng. Data* **2006**, *51*, 1389−1393.
(36) Ellis, B. L.; Makahnouk, W. R. M.; Makimura, Y.; Toghill, K.; Nazar, L. F. *Nat. Mater.* **2007**, *6*, 749–753.
(37) Recham, N.; Chotard, J.-N.; Jumas, J.-C.; Laffont, L.; Armand, M.; Tarascon, J.-M. *Chem. Mater.*, in press, doi: 10.1021/cm9021497.
(38) Barker, J.; Saidi, M. Y.; Swoyer, J. L. Lithium metal fluorophosphate materials and preparation thereof. US patent 2001008132, international patent WO2001084655, **2001**.
(39) Barker, J.; Saidi, M. Y.; Swoyer, J. L. *Electrochem. Solid-State Lett.* **2003**, *6*, A1–A4.
(40) Barker, J.; Saidi, M. Y.; Swoyer, J. L. *J. Electrochem. Soc.* **2004**, *151*, A1670–A1677.
(41) Barker, J.; Saidi, M. Y.; Gover, R. K. B.; Burns, P.; Bryan, A. *J. Power Sources* **2007**, *174*, 927–931.
(42) Yakubovich, O. V.; Karimova, O. V.; Melnikov, O. K. *Acta. Crystallogr. C* **1997**, *C53*(4), 395–397.
(43) Padhi, A. K.; Manivannan, V.; Goodenough, J. B. *J. Electrochem. Soc.* **1998**, *145*, 1518–1520.
(44) Padhi, A. K.; Nanjundaswamy, K. S.; Masquelier, C.; Okada, S.; Goodenough, J. B. *J. Electrochem. Soc.* **1997**, *144*, 1609–1613.
(45) Goodenough, J. B.; Kim, Y. *Chem. Mater.*, in press, doi: 10.1021/cm901452z.
(46) Groguennec, L.; Marx, N.; Carlier, D.; Wattiaux, A.; Bourgeois, L.; Kubiak, P.; LeCras, F.; Delmas, C. Structure and electrochemical behaviour in lithium-ion batteries of $LiFePO_4OH$ and its proton ion-exchanged derivative $FePO_4.H_2O$. *ACS meeting CRM-100*, Cleveland, OH, May 20−23, **2009**.
(47) Sebastian, L.; Gopalakrishnan, J.; Piffard, Y. *J. Mater. Chem.* **2002**, *12*, 374–377.
(48) Recham, N.; Chotard, J.-N.; Dupont, L.; Delacourt, C.; Walker, W.; Armand, M.; Tarascon, J.-M. *Nat. Mater.*, in press, doi: 10.1038/nmat2590.
(49) Wildner, M.; Giester, G. *Neues Jahrb. Mineral., Monat.* **1991**, 296–306.
(50) Barpanda, P.; Recham, N.; Chotard, J.-N.; Djellab, K.; Wesley, W.; Armand, M.; Tarascon, J.-M. *J. Mater. Chem.*, in press, doi: 10.1039/b922063a.
(51) Barpanda, P.; Recham, N.; Boulineau, A.; Djellab, K.; Armand, M.; Tarascon, J.-M. *Chem. Mater.*, in preparation.
(52) Nam, K. T.; Kim, D. W.; Yoo, P. J.; Chiang, C. Y.; Meethong, N.; Hammond, P. T.; Chiang, Y.-M.; Belcher, A. M. *Science* **2006**, *312*, 885–888.
(53) Lee, Y.-J.; Yi, H.; Kim, W. J.; Kang, K.; Yun, D. S.; Strano, M. S.; Ceder, G.; Belcher, A. M. *Science* **2009**, *324*, 1051–1055.